Supporting Information

Ground- and Excited-States Characteristics
in Photovoltaic Polymer N2200

Guanzhao Wen [a,†] , Xianshao Zou [b,†], Rong Hu [c], Jun Peng [a], Zhifeng Chen [a], Xiaochuan He [d], Geng Dong [e,f,*] and Wei Zhang [a,*]

[a] School of Physics and Materials Science, Guangzhou University, Guangzhou 510006, China

[b] Division of Chemical Physics, Lund University, Lund 22100, Sweden

[c] School of Materials Science and Engineering, Chongqing University of Arts and Sciences, Chongqing 402160, China

[d] Songshan Lake Materials Laboratory, Dongguan 523808, China

[e] Department of Biochemistry and Molecular Biology, Shantou University Medical College, Shantou 515041, China

[f] Medical Informatics Research Center, Shantou University Medical College, Shantou 515041, China

[†] These authors contributed equally to this work.

[*] Correspondence: gdong@stu.edu.cn (G.D.); wzhang@gzhu.edu.cn (W.Z.)

Tel.: +86-187-3110-6711 (G.D.); +86-136-4279-2676 (W.Z.)

Main Contents

Figure S1. The experimental (black lines) and simulated absorption spectra of N2200 in CB solution; the simulation was performed by TD-DFT at the level of B3LYP/6-311G(d,p) and a Gaussian function with a full width at half-maximum of 0.45 eV was used. All spectra have been normalized.

From Supporting Information Figure S1, we find that the main absorption peak of the simulated absorption spectrum, which corresponds to $S_0 \rightarrow S_1$ transition, is red-shifted with the increase of the number of repetition units. This suggests the number of repetition units on the N2200 chain can influence the absorption properties of N2200, which is one of the key factors determining the performance of polymer solar cells.

A polymer chain is usually composed of many chromophores, which determined the optical properties of polymers. From TD-DFT calculations, we find that the electron densities of LUMO and HOMO are distributed on each repeating unit evenly when n < 4, while for longer oligomers (n > 4), the electron densities are localized on several repeating units. Meanwhile, the red-shift of the simulated absorption spectrum is small when n > 4. By comparing the absorption spectra of polymer with the simulated absorption of oligomers, we deduce a chromophore in a polymer chain contains at least four repeating units.

Understanding the absorption properties of oligomers with the different numbers of repeat units is helpful to design novel polymers with optimized optical properties for solar energy conversion.
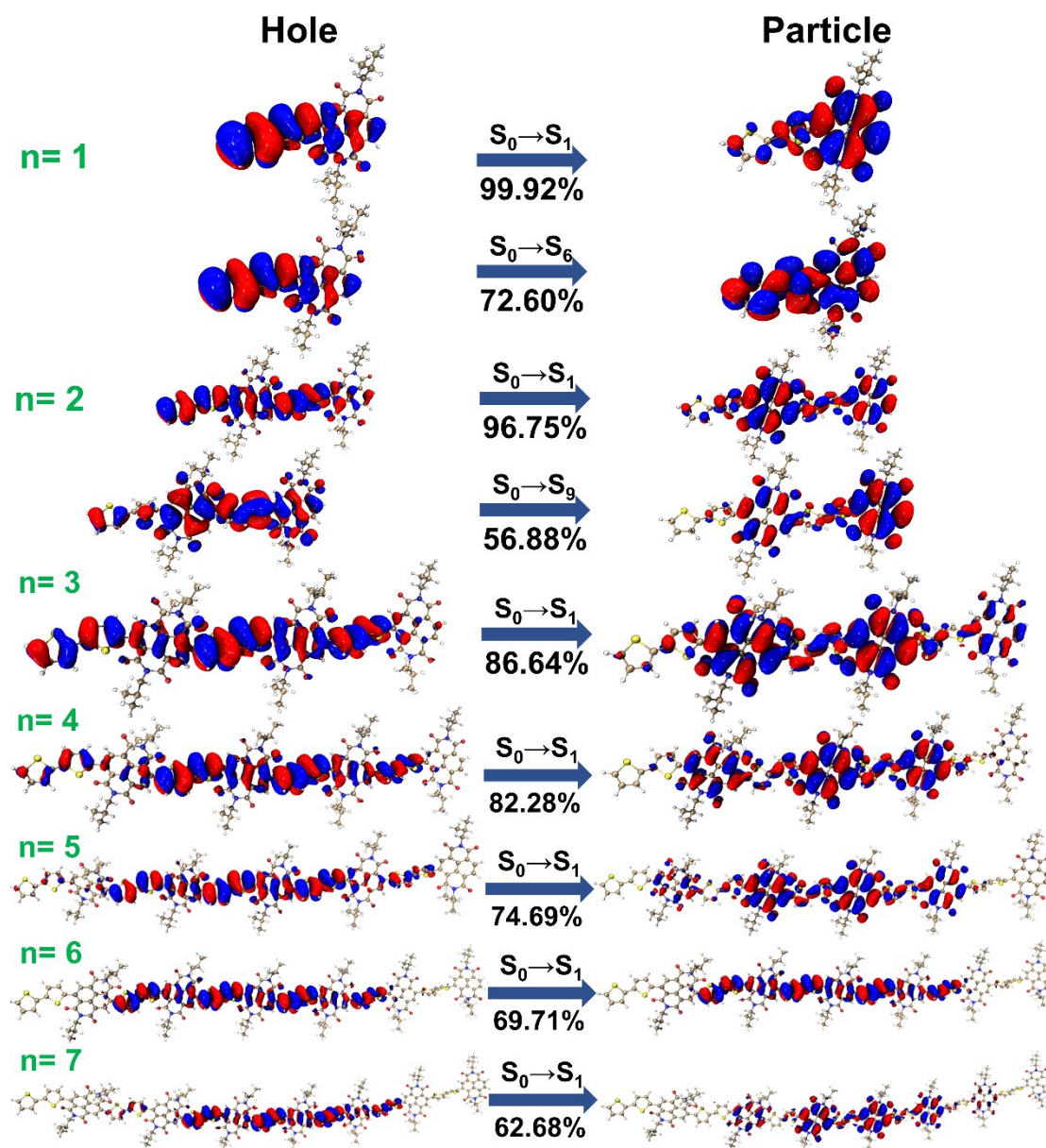
Figure S2. Computed natural transition orbital pairs of N2200 oligomers with various repeating units by TD-DFT at the level of B3LYP/6-311G(d,p). The isosurface value was set at 0.01 a.u. *n* is the number of repeating units.

~700 nm   **~390 nm**

n= 1

n= 2

n= 3

n= 4

n= 5

n= 6

n= 7
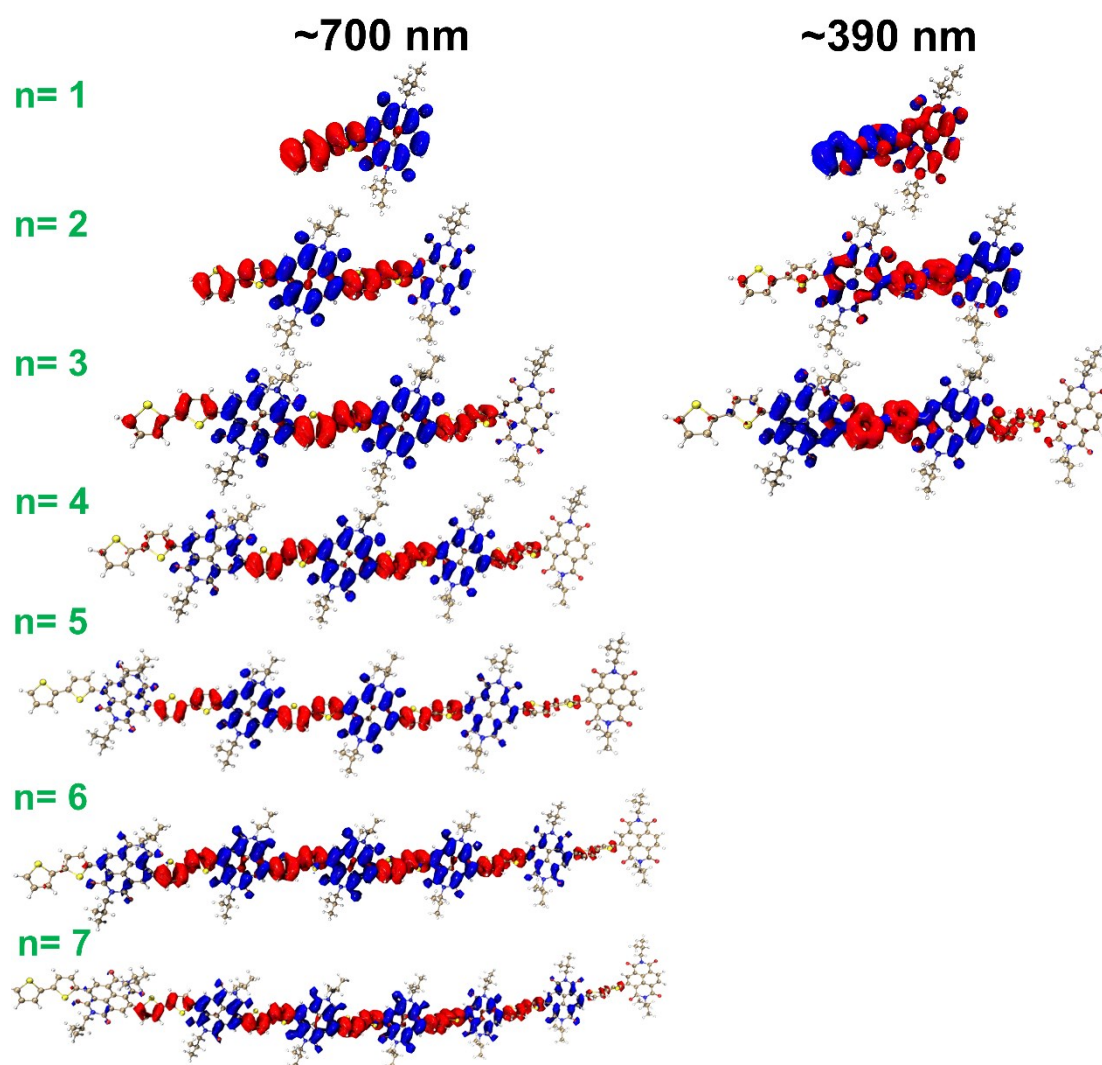
Figure S3. The overlap of electron-hole isosurface density maps of absorption peaks at around 390 nm and 700 nm of N2200 oligomers with various repeating units by TD-DFT at the level of B3LYP/6-311G(d,p). The isosurface value was set at 0.0002 a.u. n is the number of repeating units.
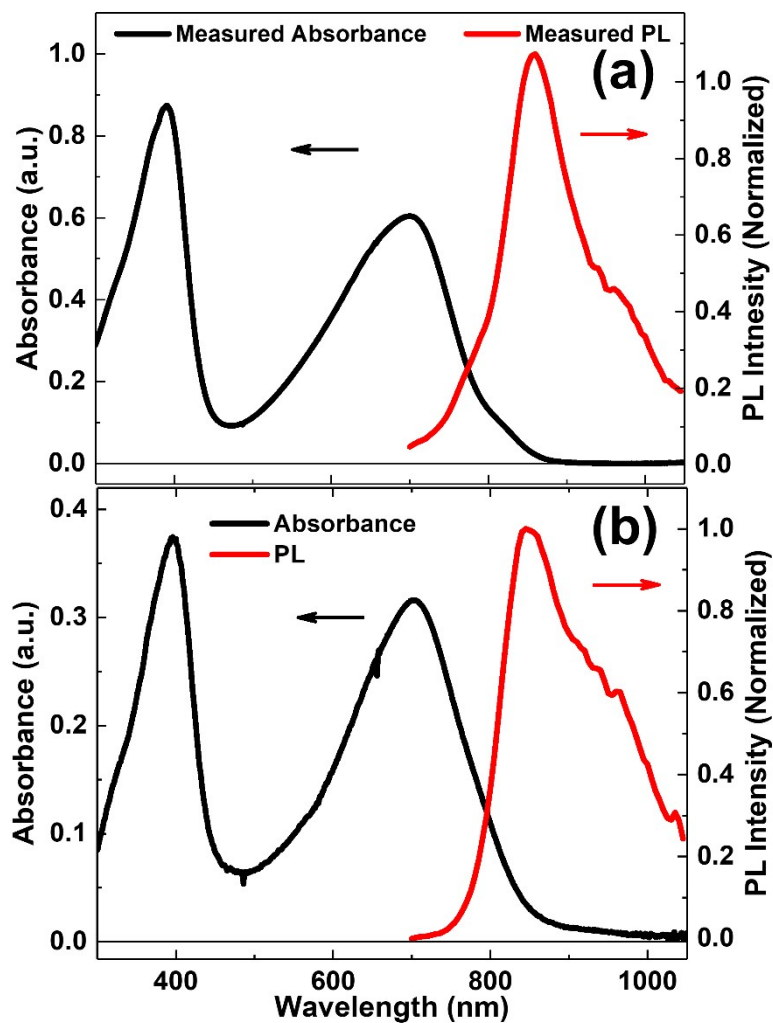
Figure S4. (a) The experimental (solid lines) and simulated (dot line) absorption and photoluminescence (PL) spectrum of N2200 in chlorobenzene solution; the simulation was performed by TD-DFT at the level of B3LYP/6-311G(d,p) and a Gaussian function with a full width at half-maximum of 0.45 eV was used. (b) Steady-state absorption (black line) and PL (red line) spectrum of N2200 thin film. The excitation wavelength for PL measurements of N2200 solution and film is 532 nm.
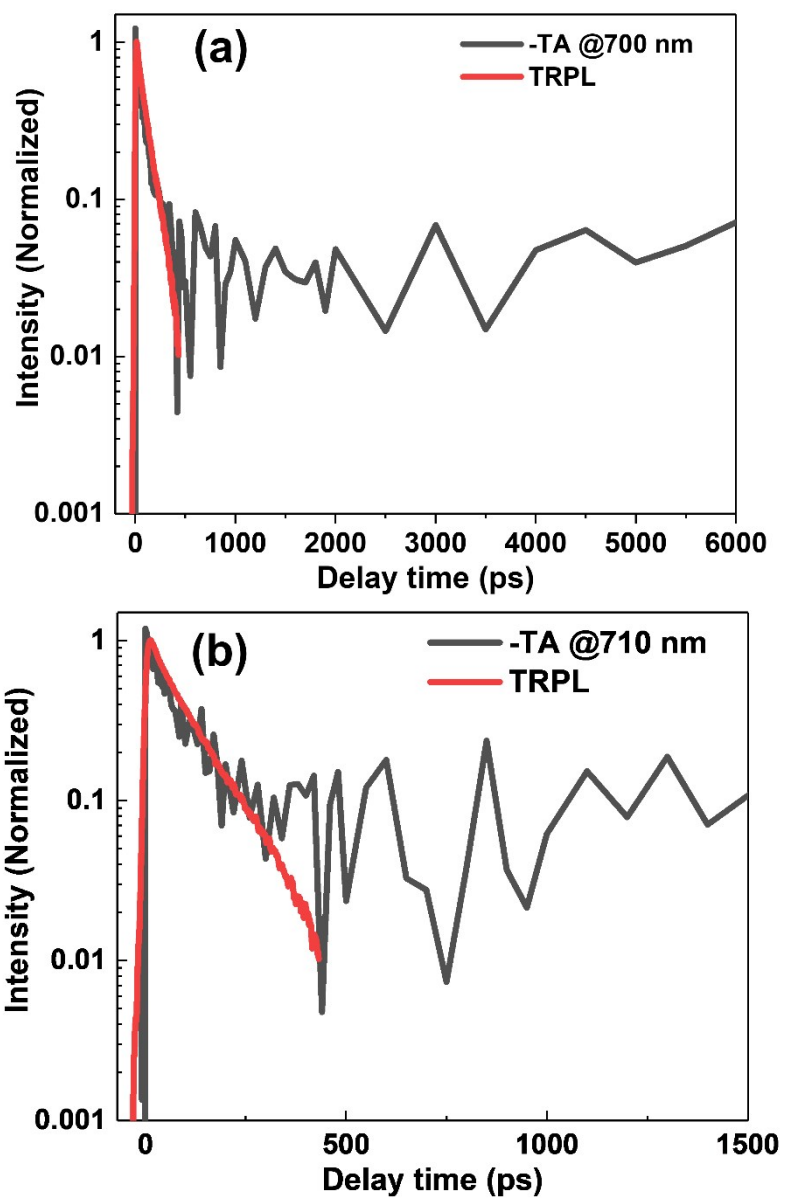
Figure S5. Comparison of TRPL kinetics and TA bleaching kinetics in N2200 (a) CB solution and (b) thin-film.
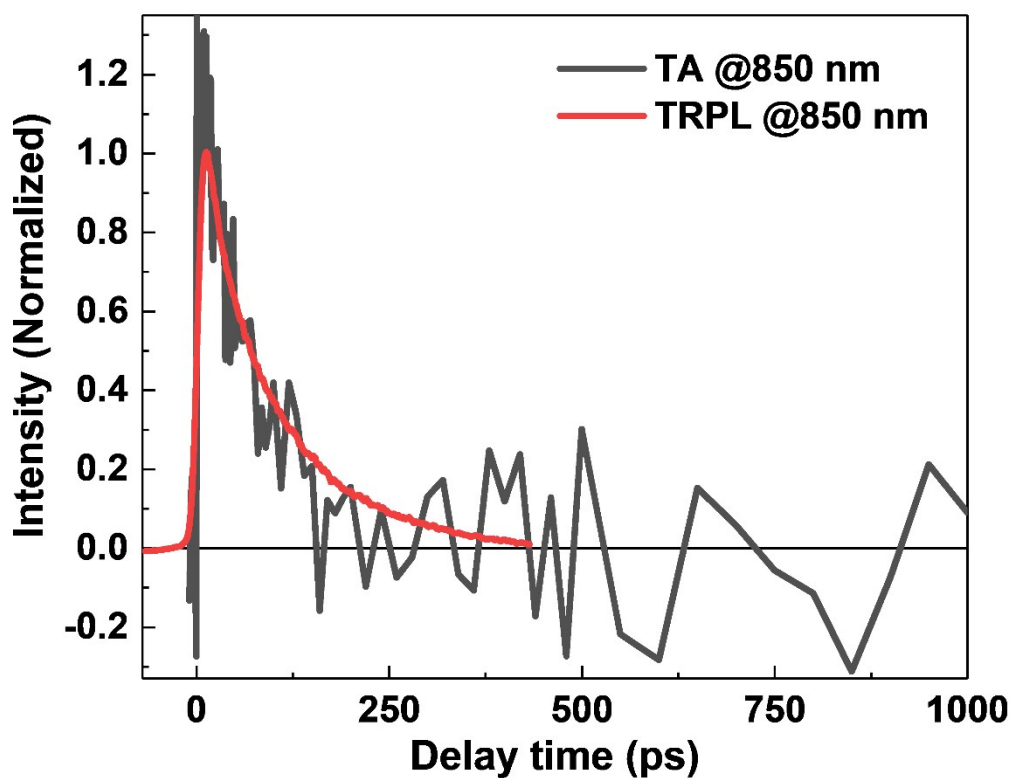
Figure S6. Comparison of the TRPL and TA kinetics in the N2200 thin-film.
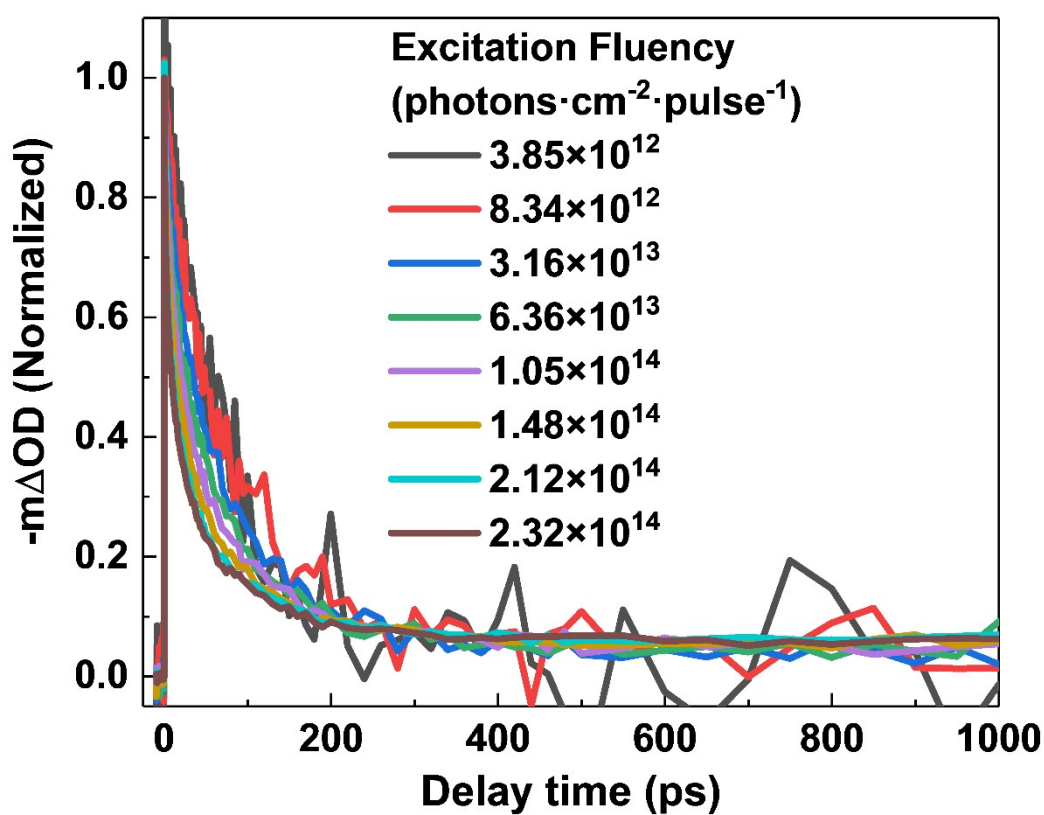
Figure S7. The normalized TA kinetics of N2200 film at a probe wavelength of 700 nm after photoexcitation at 750 nm under various excitation fluencies.
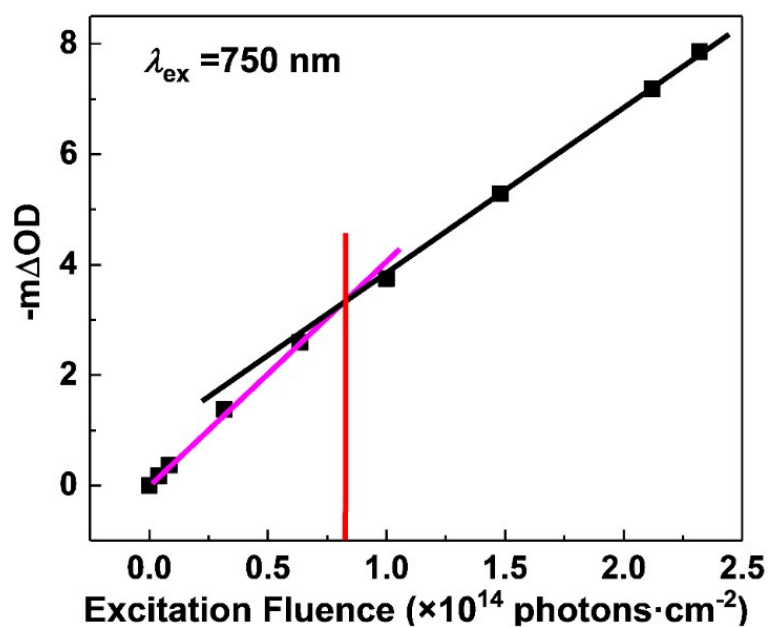
Figure S8. The excitation power-dependent maximal bleaching probed at 700 nm (Δt=0.2 ps) for N2200 film.
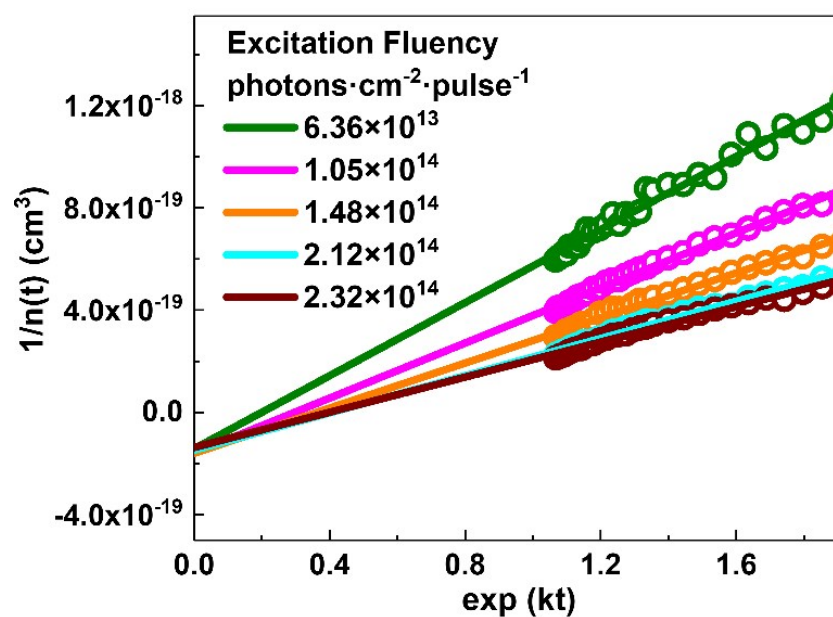
Figure S9. Reciprocal of exciton density vs exp (*k*t) of N2200 film under various excitation fluencies. The solid lines are linear fitting curves.

Computational details

Firstly, the original 3-dimensional chemical structures of the investigated N2200 oligomers were drawn by the molecular editor software (Avogadro, Version 1.2.0[1]). Since the alkyl branches (R=C_8H_{17} and $C_{10}H_{21}$) on naphthalene diimide (NDI) unit of oligomers typically have a weak influence on the molecular orbital properties of polymers[2], alkyl branches were substituted by methyl groups during the calculations to reduce the computational costs. The geometry structure optimization of the ground state of N2200 oligomers was performed using density functional theory (DFT) at the level of B3LYP/6-31G*[3,4]. After that the single point energy of the lowest twenty excited states of N2200 oligomers was calculated by the time-dependent density functional theory (TD-DFT) with a dielectric constant of 5.6968 (chlorobenzene solution) at the level of B3LYP/6-311G(d,p)[5]. The Gaussian 16 Revision B.01[6] was used to carry out all the DFT and TD-DFT calculations in this work. Moreover, the transition information such as the electron density of frontier molecular orbitals (FMOs), theoretical UV-vis absorption spectrum, major molecular orbital (MO) transitions in selected excited states, natural transition orbitals (NTOs)[7] and the overlap of electron-hole distribution[8] of excited states was performed by the Multiwfn (Version 3.7[9]) and VMD (Version 1.9.4[10]).

Table S1. Computed positions and oscillator strength (*f*) of the selected electronic transitions of N2200 oligomers with various repeating units by TD-DFT at B3LYP/6-311G(d,p) level of theory. n is the number of repeating units.

N2200-n	State	λ_{cal} (nm)	f[a]	Excitation contribution[b] (%)
N2200-1	S_1	657	0.2303	H→L (99.3)
	S_2	428	0.0077	H-1→L (77.2), H-2→L (12.4), H-3→L (6.3)
	S_3	387	0.3233	H-2→L (64.6), H-1→L (19.7), H-3→L (6.3)
	S_4	377	0.0043	H-3→L (31.6), H-5→L (22.1), H-2→L (20.7), H-6→L (8.6), H-4→L (7.9)
	S_5	370	0.0276	H-3→L (48.5), H-5→L (26.9), H-6→L (10.2), H-7→L (9.6)
	S_6	367	0.4476	H→L+1 (71.6), H-4→L (17.7)
N2200-2	S_1	727	0.8146	H→L (91.7)
	S_2	666	0.0065	H→L+1 (76.5), H-1→L (19.2)
	S_3	640	0.0072	H-1→L (62.8), H-1→L+1 (27.1), H→L+1 (8.1)
	S_4	575	0.0192	H-1→L+1 (67.0), H-1→L (14.7), H→L+1 (11.9), H→L (6.1)
	S_5	439	0.0015	H-2→L (79.1)
	S_9	392	0.3967	H→L+2 (25.3), H-5→L (19.4), H-6→L (13.8), H-2→L+1 (9.6), H-1→L+2 (6.0)
N2200-3	S_1	752	1.3847	H→L (83.9), H-1→L+1 (6.9)
	S_2	702	0.0094	H→L+1 (55.4), H-1→L (31.9), H→L+2 (7.3)
	S_3	665	0.0666	H→L+2 (51.4), H-1→L+1 (20.4), H-2→L (14.0), H-1→L (5.2)
	S_4	652	0.0109	H-1→L (34.4), H→L+1 (22.8), H-1→L+2 (13.6), H-2→L+2 (13.0)
	S_5	645	0.0113	H-2→L (34.8), H-2→L+1 (19.7), H-1→L+2 (18.6), H-1→L+1 (15.1), H→L+2 (7.5)
	S_{16}	397	0.6049	H-3→L+1 (14.6), H→L+4 (14.5), H-11→L (10.9), H→L+3 (10.5), H-9→L (8.4), H-8→L+1 (6.5)
N2200-4	S_1	768	1.9205	H→L (74.8), H-1→L+1 (10.6)
	S_2	729	0.0174	H→L+1 (48.3), H-1→L (35.4)
	S_3	695	0.1344	H→L+2 (39.8), H-1→L+1 (27.2), H-2→L (14.7), H→L+3 (11.7)
	S_4	669	0.0250	H→L+3 (38.8), H-1→L+2 (18.1), H-2→L+1 (14.0), H-3→L (8.6), H-1→L+3 (6.1), H-2→L (5.1)
	S_5	662	0.0004	H-1→L (35.6), H→L+1 (19.1), H-1→L+2 (11.0)

	S_1	774	2.4365	H→L (66.5), H-1→L+1 (13.5)
	S_2	745	0.0359	H→L+1 (42.7), H-1→L (34.5), H-1→L+2 (5.4)
N2200-5	S_3	714	0.2048	H→L+2 (34.3), H-1→L+1 (26.8), H-2→L (19.8)
	S_4	690	0.0061	H→L+3 (31.3), H-1→L+2 (23.7), H-2→L+1 (15.1), H→L+4 (14.4), H-3→L (8.1)
	S_5	667	0.0488	H→L+4 (24.7), H-1→L+3 (17.0), H-3→L+1 (11.0), H-2→L+2 (10.4), H-1→L+4 (7.3), H-4→L (7.0)
	S_1	779	2.9985	H→L (49.6), H-1→L (12.8), H→L+1 (8.7), H-1→L+1 (8.4)
	S_2	754	0.1162	H-1→L (31.6), H→L+1 (29.5), H→L+2 (10.1)
N2200-6	S_3	730	0.2761	H→L+2 (30.9), H-1→L+1 (25.0), H-2→L (19.2), H→L+3 (5.0)
	S_4	705	0.0320	H→L+3 (25.0), H-1→L+2 (21.1), H-2→L+1 (13.6), H-3→L (11.1)
	S_5	685	0.0158	H→L+5 (35.0), H-1→L+3 (21.1), H-2→L+2 (9.4), H-3→L+1 (7.6), H→L+4 (7.5), H-4→L (6.5)
	S_1	780	3.4841	H→L (54.6), H-1→L+1 (16.6), H-2→L+2 (6.5)
	S_2	762	0.2028	H→L+1 (31.5), H-1→ L (30.4), H-1→L+2 (7.8)
N2200-7	S_3	741	0.2924	H→L+2 (28.6), H-2→L (19.6), H-1→L+1 (18.2)
	S_4	719	0.0439	H→L+3 (23.9), H-1→L+2 (18.9), H-2→L+1 (16.6), H-3→L (14.0)
	S_5	697	0.0467	H→L+4 (15.2), H-1→L+3 (14.7), H-2→L+2 (14.1), H-3→L+1 (13.6), H-4→L (8.8), H-1→L+5 (6.8)

[a]Oscillator strengths. [b]H=HOMO, L=LUMO, H-1=HOMO-1, L+1=LUMO+1
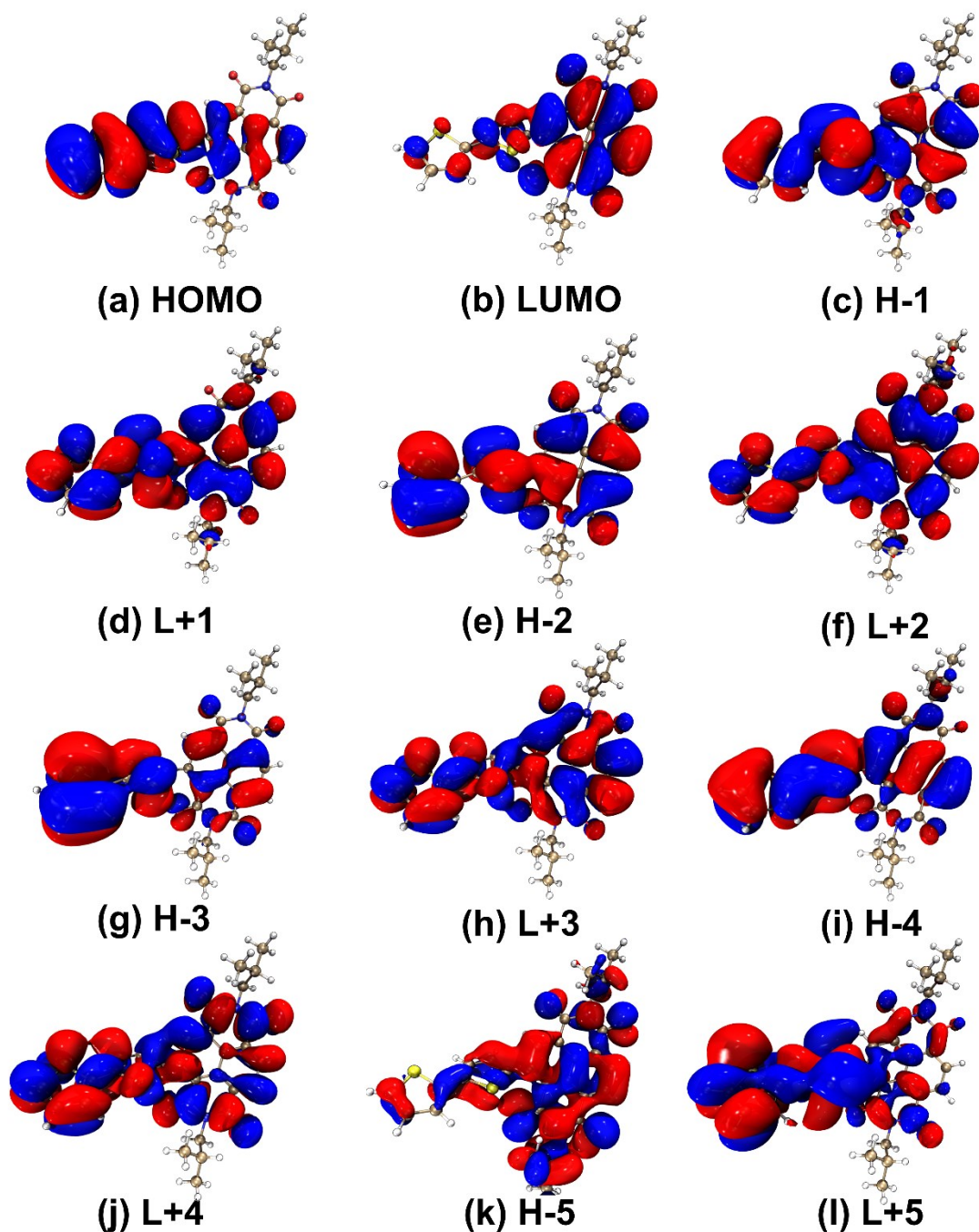
Figure S10. Electron density contours of (a) HOMO, (b) LUMO, (c) HOMO-1, (d) LUMO+1, (e) HOMO-2, (f) LUMO+2, (g) HOMO-3, (h) LUMO+3, (i) HOMO-4, (j) LUMO+4, (k) HOMO-5, (l) LUMO+5 of N2200 oligomer with one repeating unit by TD-DFT at B3LYP/6-311G(d,p) level of theory. The isosurface value was set at 0.01 a.u.
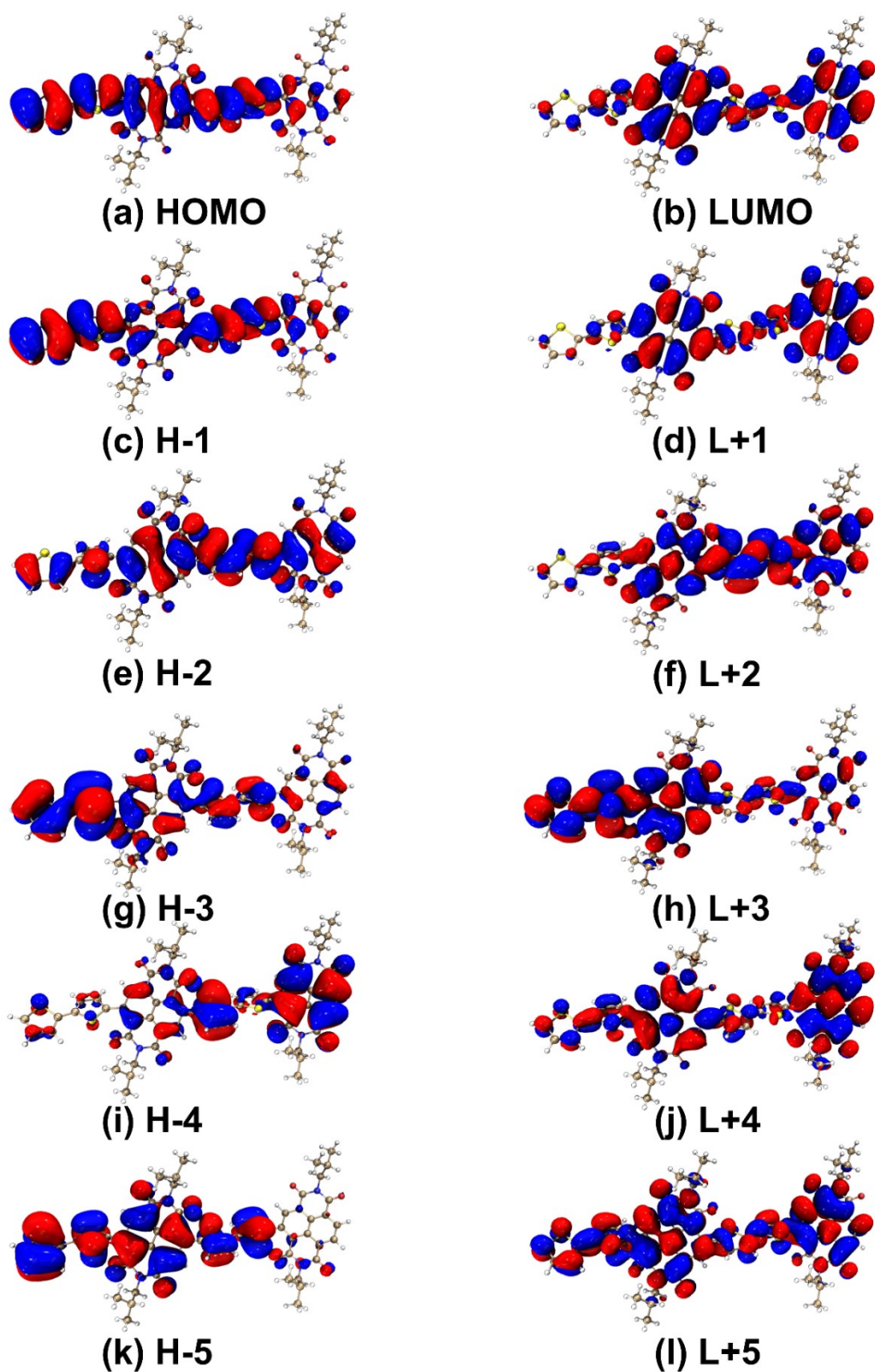
Figure S11. Electron density contours of (a) HOMO, (b) LUMO, (c) HOMO-1, (d) LUMO+1, (e) HOMO-2, (f) LUMO+2, (g) HOMO-3, (h) LUMO+3, (i) HOMO-4, (j) LUMO+4, (k) HOMO-5, (l) LUMO+5 of N2200 oligomer with two repeating units by TD-DFT at B3LYP/6-311G(d,p) level of theory. The isosurface value was set at 0.01 a.u.

(a) HOMO

(b) LUMO

(c) H-1

(d) L+1

(e) H-2

(f) L+2

(g) H-3

(h) L+3

(i) H-4

(j) L+4

(k) H-5

(l) L+5
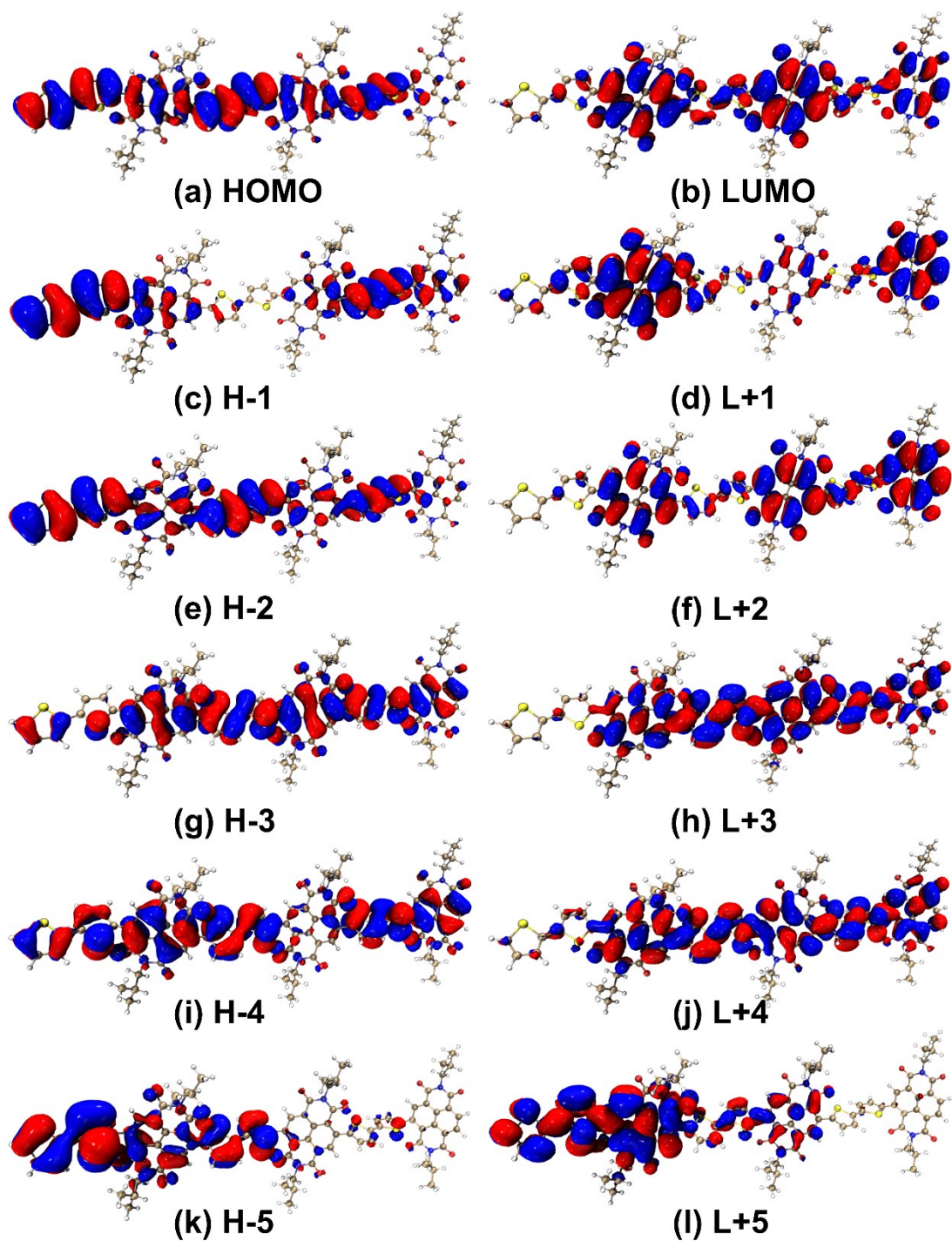
Figure S12. Electron density contours of (a) HOMO, (b) LUMO, (c) HOMO-1, (d) LUMO+1, (e) HOMO-2, (f) LUMO+2, (g) HOMO-3, (h) LUMO+3, (i) HOMO-4, (j) LUMO+4, (k) HOMO-5, (l) LUMO+5 of N2200 oligomer with three repeating units by TD-DFT at B3LYP/6-311G(d,p) level of theory. The isosurface value was set at 0.01 a.u.

(a) HOMO

(b) LUMO

(c) H-1

(d) L+1

(e) H-2

(f) L+2

(g) H-3

(h) L+3

(i) H-4

(j) L+4

(k) H-5

(l) L+5
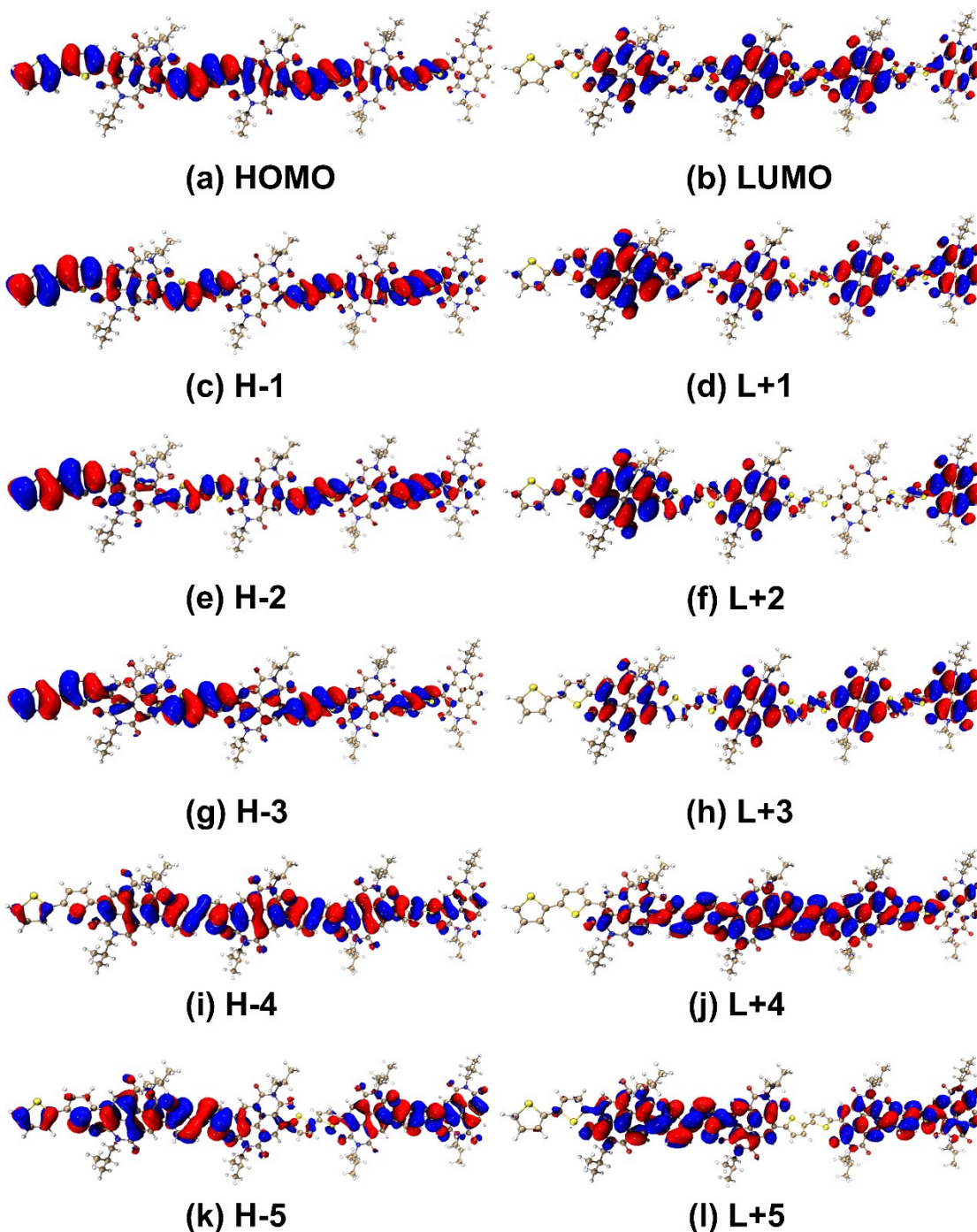
Figure S13. Electron density contours of (a) HOMO, (b) LUMO, (c) HOMO-1, (d) LUMO+1, (e) HOMO-2, (f) LUMO+2, (g) HOMO-3, (h) LUMO+3, (i) HOMO-4, (j) LUMO+4, (k) HOMO-5, (l) LUMO+5 of N2200 oligomer with four repeating units by TD-DFT at B3LYP/6-311G(d,p) level of theory. The isosurface value was set at 0.01 a.u.

(a) HOMO **(b) LUMO**

(c) H-1 **(d) L+1**

(e) H-2 **(f) L+2**

(g) H-3 **(h) L+3**

(i) H-4 **(j) L+4**

(k) H-5 **(l) L+5**
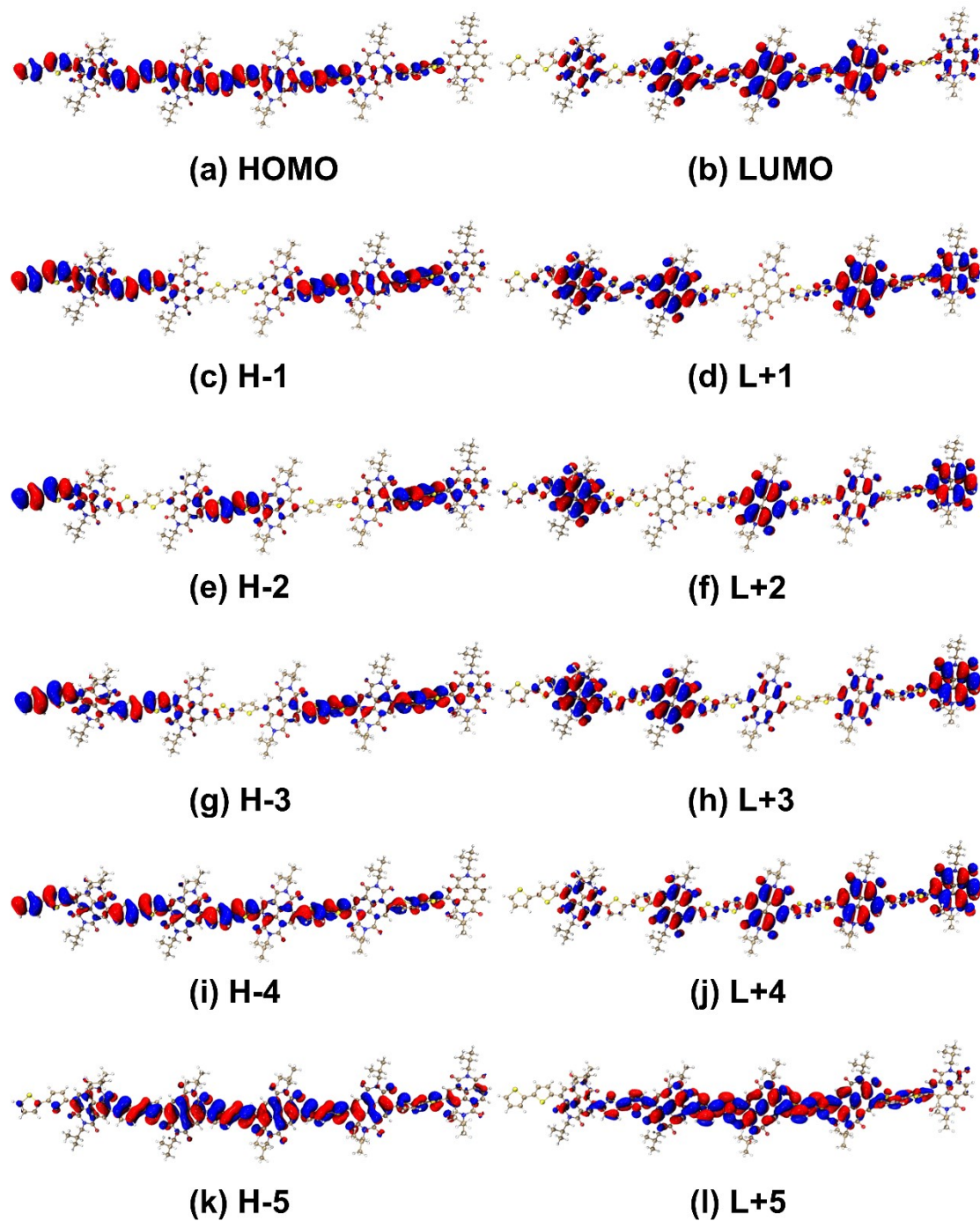
Figure S14. Electron density contours of (a) HOMO, (b) LUMO, (c) HOMO-1, (d) LUMO+1, (e) HOMO-2, (f) LUMO+2, (g) HOMO-3, (h) LUMO+3, (i) HOMO-4, (j) LUMO+4, (k) HOMO-5, (l) LUMO+5 of N2200 oligomer with five repeating units by TD-DFT at B3LYP/6-311G(d,p) level of theory. The isosurface value was set at 0.01 a.u.

(a) HOMO

(b) LUMO

(c) H-1

(d) L+1

(e) H-2

(f) L+2

(g) H-3

(h) L+3
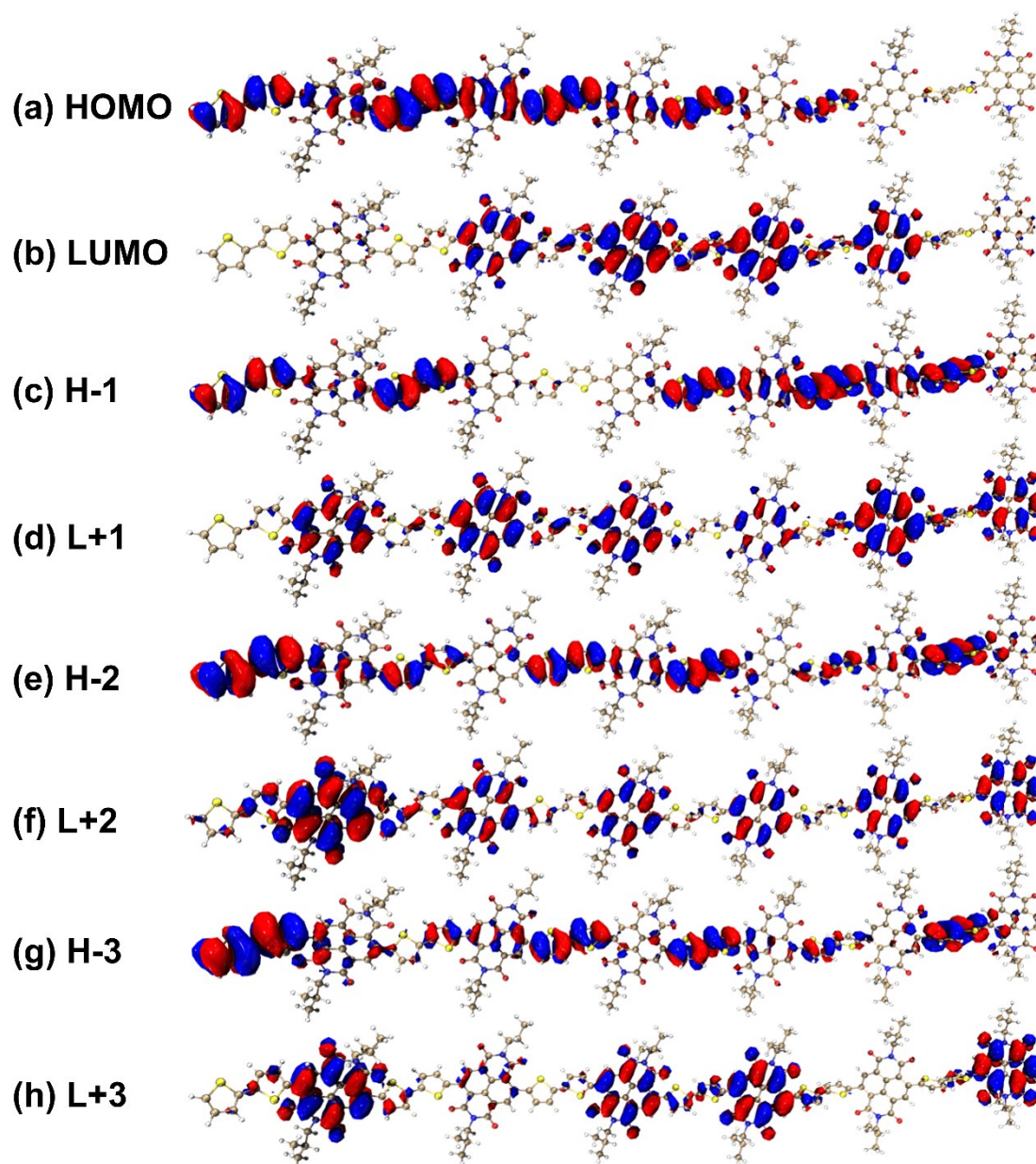
Figure S15. Electron density contours of (a) HOMO, (b) LUMO, (c) HOMO-1, (d) LUMO+1, (e) HOMO-2, (f) LUMO+2, (g) HOMO-3, (h) LUMO+3 of N2200 oligomer with six repeating units by TD-DFT at B3LYP/6-311G(d,p) level of theory. The isosurface value was set at 0.01 a.u.

(a) HOMO

(b) LUMO

(c) H-1

(d) L+1

(e) H-2

(f) L+2
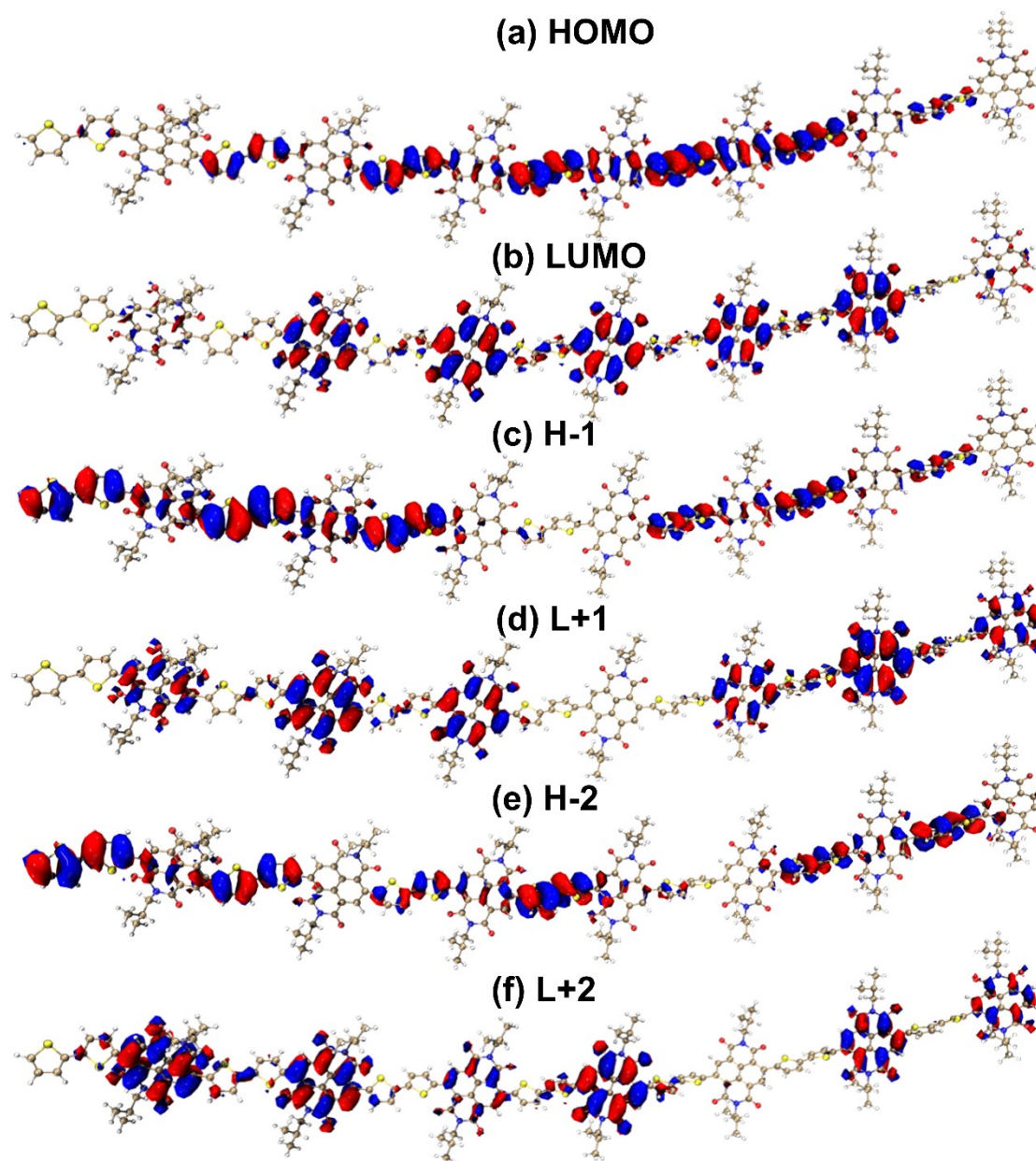
Figure S16. Electron density contours of (a) HOMO, (b) LUMO, (c) HOMO-1, (d) LUMO+1, (e) HOMO-2, (f) LUMO+2 of N2200 oligomer with seven repeating units by TD-DFT at B3LYP/6-311G(d,p) level of theory. The isosurface value was set at 0.01 a.u.

References

1.   M. D. Hanwell, D. E. Curtis, D. C. Lonie, T. Vandermeersch, E. Zurek and G. R. Hutchison, *J. Cheminform.*, 2012, **4**, 17.
2.   L. M. Tolbert, *Acc. Chem. Res.*, 1992, **25**, 561−568.
3.   P. J. Stephens, F. J. Devlin, C. F. Chabalowski and M. J. Frisch, *J. Phys. Chem.*, 1994, **98**, 11623−11627.
4.   V. A. Rassolov, J. A. Pople, M. A. Ratner and T. L. Windus, *J. Chem. Phys.*, 1998, **109**, 1223−1229.
5.   A. D. McLean and G. S. Chandler, *J. Chem. Phys.*, 1980, **72**, 5639−5648.
6.   M. J. Frisch, G. W. Trucks, H. B. Schlegel, G. E. Scuseria, M. A. Robb, J. R. Cheeseman, G. Scalmani, V. Barone, G. A. Petersson, H. Nakatsuji, et al., *Gaussian Inc.*, 2016, Wallingford, CT.
7.   R. L. Martin, *J. Chem. Phys.*, 2003, **118**, 4775−4777.
8.   Z. Liu, T. Lu and Q. Chen, *Carbon*, 2020, **165**, 461−467.
9.   T. Lu and F. Chen, *J. Comput. Chem.*, 2012, **33**, 580−592.
10.   W. Humphrey, A. Dalke and K. Schulten, *J. Mol. Graphics*, 1996, **14**, 33−38.